From linear to nonlinear response in spin glasses: Importance of mean-field-theory predictions

V. S. Zotev, G. G. Kenning, and R. Orbach
Department of Physics, University of California, Riverside, California 92521
(Received 27 December 2001; revised manuscript received 18 March 2002; published 28 June 2002)

Departures from spin-glass linear response in a single-crystal Cu:Mn (1.5 at. %) are studied for a wide range of changes in magnetic field ΔH. Three quantities, the difference $TRM-(MFC-ZFC)$, the effective waiting time t_w^{eff}, and the difference $TRM(t_w)-TRM(t_w=0)$, are examined in our analysis. Three regimes of spin-glass behavior are observed as ΔH increases. Lines in the $(T,\Delta H)$ plane, corresponding to ''weak'' and ''strong'' violations of linear response under a change in magnetic field, are shown to have the same functional form as the de-Almeida–Thouless critical line. It is suggested that the mean-field description of spin-glass dynamics, with two additional experimentally justified assumptions, predicts H/H_{AT} scaling for remanent magnetization curves. This scaling is shown to hold with high precision. Our experimental results support predictions of the mean-field theory of aging phenomena.

DOI: 10.1103/PhysRevB.66.014412 PACS number(s): 75.50.Lk, 75.40.Gb

I. INTRODUCTION

The properties of spin glasses in a magnetic field have been the subject of considerable attention. It is widely recognized that the Parisi replica-symmetry-breaking ansatz[1] provides an essentially correct equilibrium mean-field solution for the infinite-range Sherrington-Kirkpatrick (SK) model.[2] The spin-glass phase in this model is separated from the paramagnetic phase in the (T,H) plane by the de-Almeida-Thouless (AT) critical line.[3] The situation is less clear in the case of finite-dimensional short-range models. Rigorous theoretical results show viability of the mean-field approach for description of these systems,[4] but progress is impeded by significant analytical difficulties. Numerical studies have repeatedly suggested the existence of an AT-type critical line at $d=3$ and higher dimensions.[5,6] However, magnetic-field effects present a difficult challenge for computer simulations. Finite size and difficulties in equilibrating large samples do not yet allow a clear distinction between the mean-field picture and the droplet scenario.[7] Because of this, the existence of the spin-glass phase transition in a magnetic field is considered a most relevant open problem.[6]

The experimental evidence for an AT-type critical behavior remains somewhat ambiguous, and depends on the nature of a spin-glass sample. Many spin glasses have been shown to have mean-field-like phase diagrams,[8,9] with an onset of strong $MFC-ZFC$ irreversibility along a certain line. This irreversibility is usually interpreted as a sign of replica-symmetry breaking. However, real spin glasses are always out of equilibrium, and the measured AT lines are time dependent. It has been claimed that analysis of this time dependence suggests that there is no phase transition in a magnetic field in an Ising spin glass.[10] Torque measurements, on the contrary, have demonstrated that various Heisenberg spin glasses are characterized by a true spin-glass ordered phase below a transverse irreversibility line in the (T,H) plane.[11]

In general, it is hardly possible to obtain information about the *equilibrium* phase diagram directly from experiments. We show in this paper that a study of magnetic-field effects on the *nonequilibrium* dynamics can shed light on magnetic properties of the equilibrium spin-glass state.

Our motivation for this work is twofold. First, magnetic-field effects are understood fairly well within the mean-field theory, where they are derived from first principles. The minimum possible overlap $q_{min}(H)$ of two states in the presence of a magnetic field H plays an important role in this approach. Yet, as usually happens in spin-glass physics, the theoretical predictions cannot be easily related to experimentally observable phenomena. Even those models of spin-glass dynamics that are based on the mean-field-like hierarchical picture of the phase space tend to treat magnetic-field dependence phenomenologically in terms of the Zeeman energy. We show that experimental results support the mean-field description.

The second reason for this work is practical. Spin-glass relaxation properties are usually studied under a change in magnetic field. It is often believed that the subsequent response is linear in magnetic field ''for reasonably small field values[12] (say <10 G).'' We show in this paper that the very definition of what one means by ''reasonably small'' fields is impossible without knowledge of the spin-glass phase diagram. This knowledge becomes vital when results for different temperatures or different samples are compared.

The paper is organized as follows. The following Section describes a theoretical picture underlying our analysis. Section III A is devoted to a study of linear-response violations observed in magnetization measurements. In Sec. III B, the nonlinear effects are analyzed in terms of the effective waiting time. In Sec. III C, the waiting-time dependence of the measured quantities is discussed in detail. Section III D presents some new results on magnetization scaling. The last section summarizes our conclusions.

II. THEORETICAL BACKGROUND

A. Mean-field dynamics

The main obstacle to an experimental test of mean-field-theory predictions is the problem of relating experimentally accessible spin-glass dynamics to the static equilibrium properties of the spin-glass state, described by the Parisi solution. Phenomenological phase-space models have provided important insights into possible physical mechanisms for spin-

glass relaxation.[13,14] A recent theoretical breakthrough has been achieved within the mean-field theory of aging phenomena, proposed by Cugliandolo *et al.*[15–21] Because these theoretical developments have profound significance for the interpretation of our experimental results, we shall briefly review them here.

The well-known fluctuation-dissipation theorem (FDT) (Ref. 22) establishes a link between linear response of a system to an external perturbation, and fluctuation properties of the system in thermal equilibrium. Let us consider a system of N Ising spins. The autocorrelation function of states at times t and t' is given by the following expression:

$$C(t,t')=(1/N)\sum_{i=1}^{N}\langle S_i(t)S_i(t')\rangle. \tag{1}$$

The response of the system at time t to an instantaneous field at time t' is defined as follows:

$$R(t,t')=(1/N)\sum_{i=1}^{N}\delta\langle S_i(t)\rangle/\delta h(t'). \tag{2}$$

In thermodynamic equilibrium, both functions are time-translation invariant, and related by the fluctuation-dissipation theorem:

$$R_{eq}(t-t')=\frac{1}{T}\frac{\partial C_{eq}(t-t')}{\partial t'}. \tag{3}$$

Violation of this theorem in a general off-equilibrium situation is described by the function $X(t,t')\leqslant 1$:[15,16]

$$R(t,t')=\frac{X(t,t')}{T}\frac{\partial C(t,t')}{\partial t'}. \tag{4}$$

Violations of the FDT are associated with departures from linear response. A second-order nonlinearity does not appear because magnetization changes sign when the field is reversed. It has been shown[23] that presence of a third-order nonlinear response turns the fluctuation-dissipation theorem into a fluctuation-dissipation inequality. This is consistent with the fact that $X(t,t')$ in Eq. (4) is generally less than unity.

It has been suggested[15,16] that, in the limit of long times, the function $X(t,t')$ depends on its time arguments through the correlation function only, i.e., $X(t,t')=X[C(t,t')]$. A very important result of the theory is that, under the assumption of stochastic stability,[19] $X[C]$ is related to the equilibrium order parameter function $x(q)$:

$$\lim_{\substack{t,t'\to\infty\\ C=q}} X[C(t,t')]=x(q). \tag{5}$$

The function $x(q)$ is an integral of the Parisi order parameter $P(q)$,[1] which can be introduced for short-range spin glasses within the standard replica-symmetry-breaking formalism.[4] According to Eq. (5), there is a deep relationship between spin-glass dynamics and the static equilibrium properties of the spin-glass state. It implies that "in any finite-dimensional system, replica-symmetry breaking and aging in the response functions either appear together or do not appear at all" (Ref. 19).

When the aging phenomena are considered, the relevant times are $t=t_w+\tau$ and $t'=t_w$, where t_w and τ are the waiting time and observation time, respectively. The dynamical Edwards-Anderson(EA) order parameter and the minimum correlation are defined as follows:[16,21]

$$q_{EA}=\lim_{\tau\to\infty}\lim_{t_w\to\infty}C(t_w+\tau,t_w); \tag{6}$$

$$q_{min}=\lim_{\tau\to\infty}C(t_w+\tau,t_w). \tag{7}$$

Equation (6) defines q_{EA} as the value of the correlation function at the limit of validity of the fluctuation-dissipation theorem. Equation (7) reflects the property of weak ergodicity breaking in spin glasses; if the waiting time is finite and the magnetic field is zero (giving $q_{min}=0$), the system is able to escape arbitrarily far from the configuration it reached at $t=t_w$.[16]

It is well known that there are two main regimes of spin-glass relaxation. In the equilibrium, or stationary regime ($\tau\ll t_w$), the fluctuation-dissipation theorem holds and the response function depends only on τ. In the nonequilibrium, or aging regime ($\tau>t_w$), the FDT is violated and the relaxation depends on t_w for any τ. Both regimes have been observed experimentally[24] and studied numerically.[17,25] The transition from one regime to the other is marked by a peak in the relaxation rate, orresponding to strong violation of the FDT at $\tau\approx t_w$.

These effects are naturally explained within the mean-field theory of aging phenomena. In the equilibrium regime, the correlation function decreases rapidly (on the linear time scale) from 1 to q_{EA}, and $X(C)=1$. In the aging regime, the correlation function relaxes slowly from q_{EA} to q_{min}, and $X(C)<1$.[18,20] The transition from one regime to the other is directly related to replica-symmetry breaking at $q<q_{EA}$.

Magnetic susceptibility, measured in spin-glass experiments, is the integrated response. If a small magnetic field is turned on at $t=t_w$, the susceptibility measured at $t=t_w+\tau$ is given by the expression

$$\chi(t_w+\tau,t_w)=\int_{t_w}^{t_w+\tau}R(t_w+\tau,t')dt'. \tag{8}$$

In the limit of long times, the susceptibility depends on its time arguments through the correlation, i.e., $\chi=\chi(C)$. It is a linear function with a slope $-1/T$ in the equilibrium regime:

$$\chi(C)=[1-C]/T,\quad q_{EA}\leqslant C<1. \tag{9}$$

In the aging regime, the relaxing part of the susceptibility, $\chi_{ag}(C)$, is nonlinear:

$$\chi(C)=[1-q_{EA}]/T+\chi_{ag}(C),\quad q_{min}<C<q_{EA}. \tag{10}$$

The Parisi-Toulouse approximation[26] makes use of the following assumptions: the equilibrium susceptibility χ_{FC} is independent of temperature, while q_{EA} and q_{min} are func-

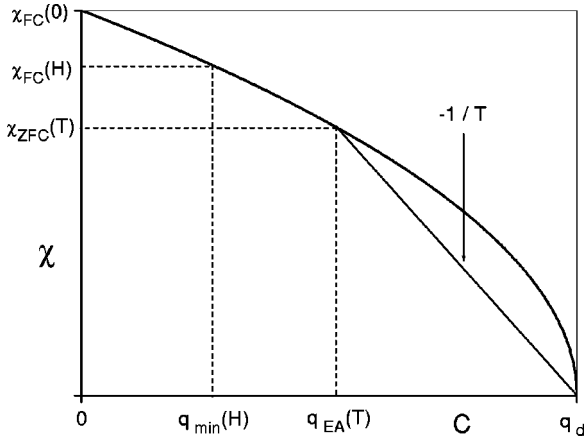

FIG. 1. A diagram of spin-glass relaxation at temperature T after magnetic field H is applied. The thick line is the master curve $\tilde{\chi}(C)$. The straight-line segment from $(q_d,0)$ to (q_{EA},χ_{ZFC}) represents the equilibrium relaxation regime. The slope is $-1/T$. The master curve segment from (q_{EA},χ_{ZFC}) to (q_{min},χ_{FC}) corresponds to the aging regime. (Cugliandolo *et al.*, Ref. 21).

tions of only temperature and magnetic field, respectively. It is also assumed that $q(x,T)=q(x/T)$.[26] The dynamical version of this approximation implies[18,21] that the function $\chi_{ag}(C)$ in Eq. (10) is both T and H independent. This means that the dependence $\chi(C)$ is universal in the aging regime, and follows a master curve $\tilde{\chi}(C)$. If the value of the susceptibility at the limit of validity of the FDT, i.e., at $C=q_{EA}$, is denoted as χ_{ZFC}, one can write the following:

$$\chi_{FC}=\chi_{FC}(H), \quad \chi_{ZFC}=\chi_{ZFC}(T). \tag{11}$$

Figure 1 exhibits the master curve $\tilde{\chi}(C)$. The quantity q_d is the initial correlation $C(t_w,t_w)$, which depends on the number of spin components. It appears instead of unity in Eqs. (9) and (10) if the spins are not Ising.

According to Fig. 1, the remanent susceptibility, $\chi_{FC}(H)-\chi_{ZFC}(T)$, is related to the difference $q_{EA}(T)-q_{min}(H)$. In order to derive a magnetic-field scaling relationship, we must introduce two additional assumptions. First, we consider relatively high temperatures and assume that the master curve $\tilde{\chi}(C)$ at low C can be approximated by a straight line. Recent measurements of both the susceptibility and the correlation[27] suggest that this approximation works well indeed. Then the triangles in Fig. 1 are geometrically similar for all allowed T and H, and the following relation holds:

$$\frac{\chi_{FC}(H)-\chi_{ZFC}(T)}{\chi_{FC}(0)-\chi_{ZFC}(T)}=\frac{q_{EA}(T)-q_{min}(H)}{q_{EA}(T)}. \tag{12}$$

Second, let us suppose that $q_{min}(H)$ is a homogeneous function of order p, that is, $q_{min}(aH)=a^p q_{min}(H)$ with some $p\neq 0$. Then, introducing the critical AT field via the relation $q_{min}[H_{AT}(T)]=q_{EA}(T)$, one can write:

$$\frac{q_{min}(H)}{q_{EA}(T)}=\frac{q_{min}[H/H_{AT}(T)]}{q_{min}(1)}. \tag{13}$$

It follows from Eqs. (12) and (13) that the remanent susceptibility, $\chi_{FC}(H)-\chi_{ZFC}(T)$, should scale as H/H_{AT}. This is a consequence of the proposed universality of $\chi(C)$ in the aging regime. We shall further discuss this issue in Sec. III D.

B. Chaotic nature of the spin-glass state

Another important issue is the chaotic nature of the spin-glass state with respect to magnetic field. It has been demonstrated numerically that a small change in external field leads to a considerable reorganization of a spin configuration.[28] The Parisi solution suggests that an average equilibrium overlap between two states at different but similar magnetic fields, $(h_1-h_2)^2N\gg 1$,[4] is equal to q_{min}, i.e., the minimum possible overlap.[29] Analysis of fluctuations around the Parisi solution, carried out by Kondor,[30] demonstrates that the correlation overlap function $C_H(r)$ for two spins i and j at a distance r behaves as

$$C_H(r)=\overline{\langle S_iS_j\rangle_H\langle S_iS_j\rangle_0}\propto\exp(-r/\xi_H). \tag{14}$$

This means that the projection of the correlation $\langle S_iS_j\rangle_H$ at field H onto the correlation $\langle S_iS_j\rangle_0$ at zero field vanishes beyond the finite characteristic length ξ_H. Near T_g and at low fields, this magnetic correlation length is simply $\xi_H=1/q_{min}(H)$. In the mean-field theory, $q_{min}(H)\propto H^{2/3}$, so that ξ_H diverges rapidly as the field goes to zero.

The behavior of the correlation function, Eq. (14), is a consequence of replica-symmetry breaking. The low-temperature spin-glass phase has an essentially infinite number of pure equilibrium states. Each of them is characterized by an infinite correlation length. These states have equal free energies per site, except for differences of the order $O(1/N)$. Only a few states with the lowest energies contribute significantly to the partition function. Because of the small energy differences, any small (but finite) amount of energy added to the system is enough to reshuffle the Boltzmann weights of the different states and thus completely reorganize the equilibrium spin configuration. Application of a magnetic field is an example of such a perturbation.

The magnetic correlation length ξ_H has the following meaning.[31] When a magnetic field H is applied to the system, the minimum possible overlap of two states is equal to $q_{min}(H)$. Consequently, all the states having overlaps $q<q_{min}$ are suppressed by the field. Their free energies increase, and they acquire the finite correlation length ξ_H. The spatial spin correlations, corresponding to these states, survive only within this range. All the other pure states are still characterized by an infinite correlation length. At the AT line, where $q_{min}=q_{EA}$, all the states have a finite correlation length, and the system becomes paramagnetic. Thus, a change in magnetic field has a randomizing effect on the spin-glass state. The ratio q_{min}/q_{EA} is a natural measure of this effect.

The chaotic nature of the spin-glass state is also reflected in the phenomenological droplet model. The magnetic correlation length is determined as an average droplet size for which the Zeeman energy is equal to the energy of the droplet excitation. It is given by the following expression:[32]

$$\xi_H \propto H^{-2/(d-2\theta)}. \quad (15)$$

Even though this result, with $d=3$ and $\theta \approx 0.2$, is similar to the result of the mean-field theory, the physics is quite different. Spin-glass properties in this model are governed by low-energy excitations of the ground state, created by coherent flipping of compact clusters of spins. It is suggested that the magnetic field H would flip all the droplets with sizes greater than ξ_H and thus destroy *all* spin-glass correlations beyond this length scale. Therefore, at any nonzero field, there is only a paramagnetic state with the finite correlation length ξ_H.

In both these approaches, the chaotic nature of the spin-glass state with respect to magnetic field leads to departures from linear response as ΔH increases.

III. EXPERIMENTAL RESULTS AND ANALYSIS

The purpose of this paper is to study violations of the fluctuation-dissipation theorem under an increasing field change ΔH. According to Eq. (5), aging dynamics of the spin-glass state are ultimately determined by its static equilibrium properties. Any violation of the FDT contains information about replica-symmetry breaking. Therefore, studies of the gradual deviation from linear response as ΔH increases can provide insight into the nature of the spin-glass phase diagram. Direct experimental determination of the correlation function, Eq. (1), requires sophisticated measurements of the magnetic noise spectrum.[27] Instead, we make use of quantities that can be obtained from magnetic-susceptibility measurements. The first quantity of interest is the difference between the thermoremanent magnetization (TRM) and the remanence, measured in zero-field-cooled (ZFC) magnetization experiments: $TRM-(MFC-ZFC)$. It has been shown[33] that, within the linear regime, this quantity is zero, provided that all three magnetizations are measured at the same time after the initial quench. The second quantity of interest is the effective waiting time t_w^{eff}, defined as the value of the observation time τ, at which the relaxation rate $S(\tau)=-\partial TRM(\tau,t_w,\Delta H)/\partial \ln \tau$ has a maximum. It has been argued[34] that within the linear-response regime, $t_w^{eff} \approx t_w$, so that the peak in $S(\tau)$ is essentially unaffected by a small magnetic-field change. The third quantity we study experimentally is the difference $TRM(t_w)-TRM(t_w=0)$. It describes a change in the measured magnetization as a result of the waiting time, and thus allows closer examination of aging effects.

Most experiments were performed on a single crystal of Cu:Mn (1.5 at. %), a typical Heisenberg spin glass with a glass temperature of about 15.2 K. Results of conventional studies of the phase diagram for this sample will be reported elsewhere. A commercial MPMS magnetometer by Quantum Design was used for all the measurements.

A. Measurements of *TRM*, *MFC*, and *ZFC*

Figure 2 exhibits dependences of TRM, $MFC-ZFC$, and their difference, on the field change ΔH. In the TRM experiment, the sample is cooled down to the measurement temperature $T=12.0$ K, in the presence of the field $H=\Delta H$, which is then cut to zero. In the ZFC experiment, the sample is cooled at zero field, and then the field $H=\Delta H$ is applied. All data points were taken at the same short observation time $\tau \approx 40$ s with zero waiting time, and an effective cooling time of about 600 s. Error bars are smaller than the symbol sizes. The same will apply to all figures without error bars.

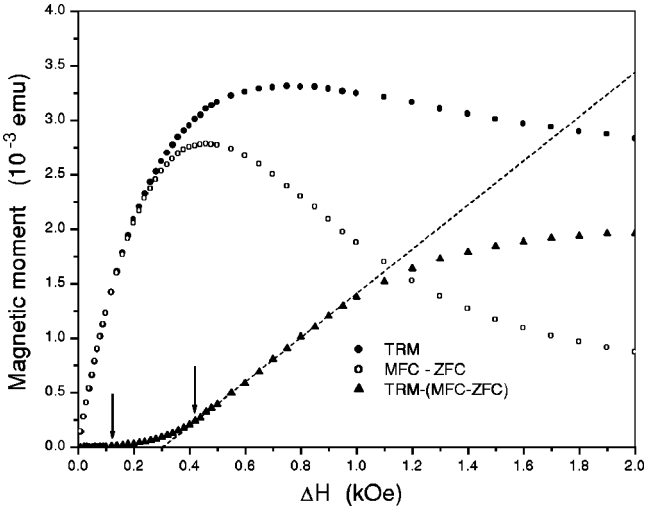

FIG. 2. The remanent magnetic moments, TRM and $MFC-ZFC$, as well as their difference, measured at $T=12.0$ K $=0.79T_g$ and $t_w=0$. The two arrows indicate the characteristic field changes, $\Delta H_1 \approx 120$ Oe and $\Delta H_2 \approx 420$ Oe, for the weak and strong linear-response violations, respectively.

According to Fig. 2, three different types of spin-glass behavior can be distinguished for different ranges of magnetic-field variation ΔH. For field changes from $\Delta H=0$ to $\Delta H_1 \approx 120$ Oe, the difference $TRM-(MFC-ZFC)$ is zero to within our experimental accuracy. Between ΔH_1 and $\Delta H_2 \approx 420$ Oe, there are weak deviations from linear response. At $\Delta H=\Delta H_2$, corresponding approximately to the peak in the $MFC-ZFC$ remanence, violation of linear response becomes strong, and the difference $TRM-(MFC-ZFC)$ is a linear function of ΔH with a large slope.

Temperature dependences of the characteristic field changes, ΔH_1 and ΔH_2, are exhibited in Figs. 3 and 4. The figures also display the critical AT line, determined for the same sample at the same observation and cooling times, using the onset of strong $MFC-ZFC$ irreversibility as the signature of the spin-glass phase transition. We assume that this dynamical line approximates the equilibrium AT line for infinite waiting time. The difference $MFC-ZFC$ in Fig. 2 is not zero at the AT field of ≈ 1400 Oe because transverse freezing above the AT line leads to a weak longitudinal irreversibility.[35]

One can see from Fig. 3 that all three lines in the $(T,\Delta H)$ plane have the same functional form, $T_g-T=a\Delta H^{2/3}$, typical of the equilibrium AT critical line[3] in the SK model. Moreover, the two linear-response violation lines, $\Delta H_1(T)$ and $\Delta H_2(T)$, determine dynamical transition temperatures that are very close to the actual glass temperature T_g. It would thus be incorrect to say that the critical AT-type line

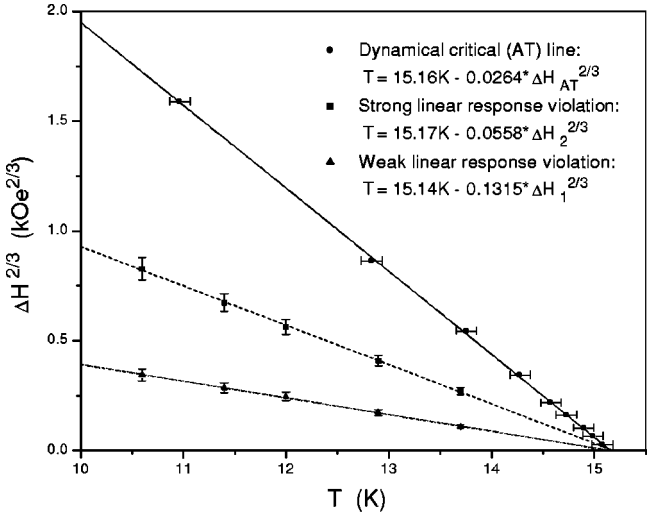

FIG. 3. The dynamical AT line $\Delta H_{AT}(T)$, the strong linear-response violation line $\Delta H_2(T)$, and the weak linear-response violation line $\Delta H_1(T)$, determined from the linear fits to experimental data, plotted as $\Delta H^{2/3}$ vs T.

plays a role at high fields only. Our results demonstrate that this line manifests itself dynamically even at very low fields. A characteristic field change for a given degree of linear response violation appears to be a constant fraction of the AT field. It means, from a practical point of view, that results obtained at different temperatures can be directly compared only if they have the same $\Delta H/H_{AT}(T)$ ratio.

A comment should be made at this point. It has been argued[36] that a $T \propto H^{2/3}$ dependence for critical lines is not a unique feature of the mean-field theory. A similar power law could be obtained from purely dynamical considerations without using the concept of the spin-glass phase

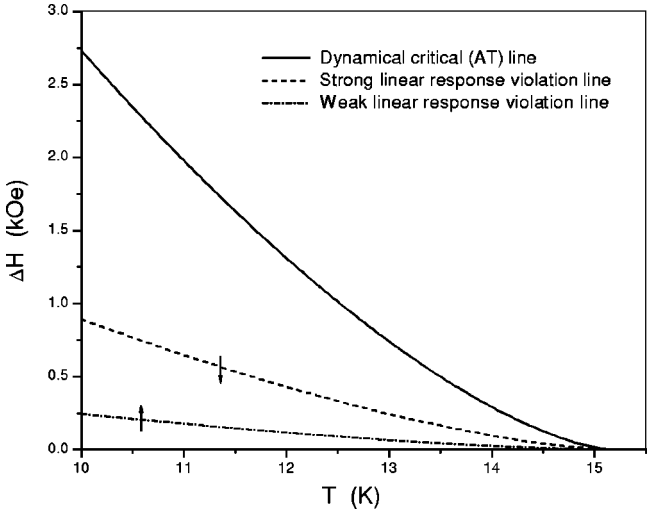

FIG. 4. The same lines as in Fig. 3, but plotted as $\Delta H(T)$. Note that the two linear-response violation lines below the AT line represent a dynamic crossover from one relaxation regime to the other. They are *not* features of an equilibrium phase diagram. The arrows indicate directions in which these lines change as the waiting time t_w increases.

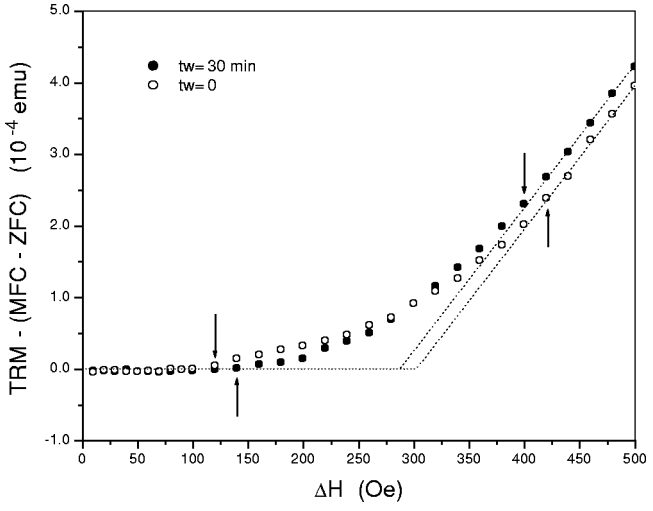

FIG. 5. The function $TRM-(MFC-ZFC)$, describing violation of linear response, for $t_w=30$ min and $t_w=0$. The second and the third arrows from the left indicate, respectively, the higher value of ΔH_1 and the lower value of ΔH_2 for the longer waiting time.

transition.[36] A dynamical freezing line, $T_f(H,\omega)$, appears in the droplet model as well.[32] In the present analysis, we do not rely on the existence of the $H^{2/3}$ dependence by itself. Our argument is based on the fact that the experimental AT and linear-response violation lines have the *same* functional form, as illustrated in Figs. 3 and 4. This result suggests that there is a close relationship between the static and dynamic properties of the spin-glass state, assuming that the measured AT line is related to the equilibrium one.

Of course, measured values of the characteristic field changes depend on both the waiting time and the observation time. This point is illustrated in Fig. 5 where values of $TRM-(MFC-ZFC)$ are plotted for $t_w=0$ and $t_w=30$ min. As the waiting time becomes larger, ΔH_1 increases, while ΔH_2 decreases. Thus, longer equilibration times make the system less susceptible to external perturbations, but only up to a certain limit. This issue will be discussed further in Sec. III C.

B. Measurements of the effective waiting time

Let us now turn to a discussion of the effective waiting time t_w^{eff}. Figure 6 exhibits dependence of $\log_{10}(t_w^{eff})$ on the magnetic-field change ΔH for three different waiting times: $t_w=30$ min, 5 min, and 0 min. The temperature is the same as in Fig. 2. The inset displays an example of the experimental $S(\tau)$ curve. The position of its maximum is the effective waiting time t_w^{eff}.

In Fig. 6, one can easily discern three regimes of the FDT violation, corresponding to the three regimes of deviation from linear response seen in Fig. 2.

As the magnetic-field change ΔH increases from zero up to about 100 Oe, the effective waiting time decreases only slightly. This means that the FDT holds for observation times less than $t_w^{eff} \approx t_w$. Of course, if the waiting time is short, t_w^{eff} is determined by the cooling procedure.

In the interval from 100 Oe to about 400 Oe, the effective waiting time drops sharply, and the field dependence of

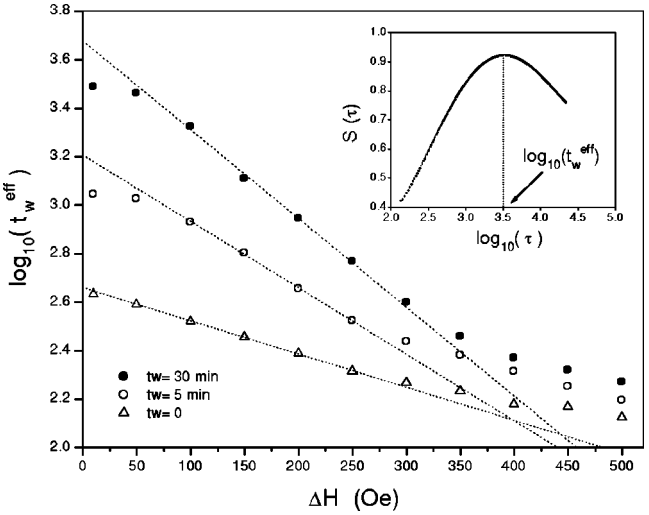

FIG. 6. Logarithm of the effective waiting time t_w^{eff} as a function of ΔH, measured at $T=12.0$ K$=0.79$ T_g for three waiting times. The dotted lines are linear fits in the interval 100–250 Oe. The inset exhibits the logarithmic relaxation rate $S(\tau)$ for $t_w=30$ min and $\Delta H=10$ Oe.

its logarithm is linear. In this case, nonequilibrium behavior appears much earlier, and the FDT holds only at short times $\tau \ll t_w^{eff} \ll t_w$. This corresponds to the weak departure from linear response between ΔH_1 and ΔH_2 in Fig. 2.

When the field change exceeds 400 Oe, the FDT is strongly violated. One can see from Fig. 6 that, in this regime, the curves for long waiting times approach the curve for zero waiting time, and the waiting time dependence almost disappears. This situation corresponds to the strong deviation from linear response at short observation times above ΔH_2 in Fig. 2. Therefore, the break from the linear dependence of $\log_{10}(t_w^{eff})$ on ΔH, observed at large field changes, is directly related to strong nonlinearity in spin-glass response. The effective waiting-time in this case is determined primarily by the zero waiting time results, defined by the experimental protocol.

The waiting-time dependence in Fig. 6 supports the conclusion drawn from Fig. 5 that an increase in waiting-time leads to an expansion of the linear response region to higher values of ΔH. An increase in the observation time τ has the opposite effect. The field dependence is more pronounced at longer times. This accounts for the fact that the characteristic field changes, extracted from the effective waiting-time experiments (Fig. 6), seem to be lower than those obtained from the short-time magnetization measurements (Fig. 5). Another interesting feature of our results is that the dependence of $\log_{10}(t_w^{eff})$ on ΔH for $t_w=0$, determined exclusively by the cooling procedure, does not exhibit the low-field plateau seen at longer waiting-times. This behavior is analyzed in Sec. III C.

Temperature dependence of the effective waiting-time is exhibited in Figs. 7 and 8, where $\log_{10}(t_w^{eff})$ vs ΔH data for $t_w=30$ min are plotted for four different temperatures. The results for the smallest field change of 10 Oe are not exactly the same because the effective cooling time increases as the measurement temperature is lowered. It is quite evident from

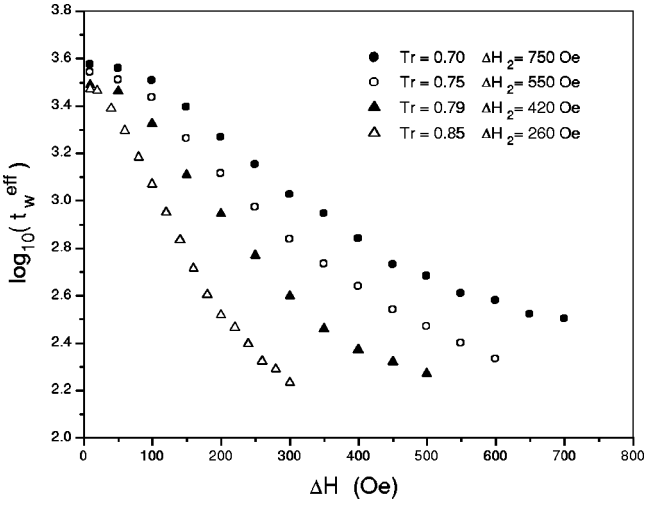

FIG. 7. Logarithm of the effective waiting-time t_w^{eff} measured as a function of ΔH for $t_w=30$ min at four temperatures: $T_r=T/T_g=0.70$, 0.75, 0.79, and 0.85. Note the similarity in shape and pronounced difference in magnetic-field scales.

Fig. 8, however, that the four curves scale rather well together if plotted vs $\Delta H/\Delta H_2$. This means that the critical AT line sets a characteristic magnetic-field scale at any temperature below T_g, and that it plays an important role for *all* aspects of spin-glass dynamics.

C. Waiting-time dependence of ΔH_1 and ΔH_2

Waiting-time dependences of the characteristic field changes, corresponding to the weak and strong linear-response violations, deserve special attention. Our experimental results, exhibited in Figs. 5 and 6, suggest that ΔH_1 increases with t_w, while ΔH_2 diminishes.

In order to check this conclusion, we have measured field dependence of the thermoremanent magnetization,

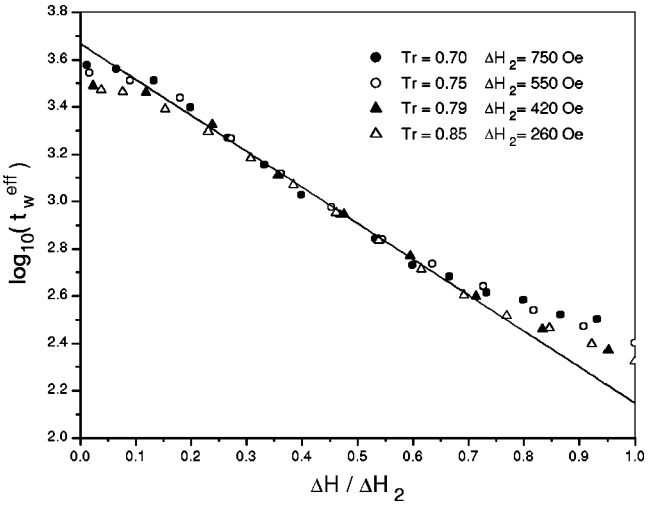

FIG. 8. The experimental results of Fig. 7, plotted vs $\Delta H/\Delta H_2$. The critical field change ΔH_2, corresponding to strong violation of linear response, is proportional to the AT field $H_{AT}(T)$. The straight line is a guide for the eye.

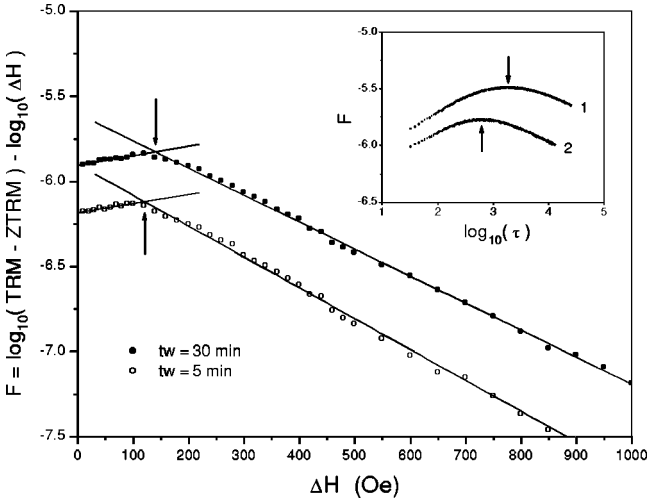

FIG. 9. Logarithm of the normalized increase in the thermoremanent magnetization $(TRM-ZTRM)/\Delta H$ as a function of ΔH at a constant observation time $\tau=40$ s. The waiting-times are $t_w=30$ min and $t_w=5$ min. The arrows indicate points where nonlinearity appears. The inset displays the same quantity, but as a function of $\log_{10}(\tau)$ at a constant $\Delta H=10$ Oe. The curve 1 is for $t_w=105$ min, and the curve 2 is for $t_w=17$ min.

$TRM(\tau,t_w,\Delta H)$, for three different waiting-times: $t_w=30$ min, 5 min, and 0. The measurement temperature was $T=12.0$ K$=0.79T_g$. For convenience, we shall refer to the zero-waiting-time dependence as $ZTRM(\tau,\Delta H)$. This relaxation is governed by the cooling process and not by the waiting-time. The absence of the low-field plateau in the field dependence of the effective waiting-time for $t_w=0$ in Fig. 6 suggests that the $ZTRM$ is not characterized by a single well defined time scale.

Figure 9 exhibits logarithm of the ratio $(TRM-ZTRM)/\Delta H$ as a function of ΔH. Two different types of behavior can be clearly distinguished. The ratio increases as long as the field change is less than about 120 Oe, and decreases at higher ΔH. The field dependence of its logarithm can be approximated by straight lines in both regimes. The results in Fig. 9 can be understood if we compare them with the data in Fig. 6. At low field changes, the effective waiting-time for the $ZTRM$ decreases more steeply with increasing ΔH than the effective waiting-time for the TRM, which has a plateau in this region. The decay of the $ZTRM$ becomes faster in time, and the ratio $(TRM-ZTRM)/\Delta H$, measured at fixed observation time, increases with ΔH. At higher magnetic-field changes, the drop in the effective waiting-time for the TRM is greater than for the $ZTRM$. As a result, the ratio $(TRM-ZTRM)/\Delta H$ decreases. According to Fig. 9, the transition from one regime to the other occurs at the higher magnetic-field change for the longer waiting-time. This observation supports our conclusion that the plateau in the field dependence of the effective waiting-time broadens as the system equilibrates.

The inset in Fig. 9 displays the logarithm of the $(TRM-ZTRM)/\Delta H$ as a function of observation time at constant $\Delta H=10$ Oe. Its waiting-time dependence is readily understandable: the system remains longer in the quasiequilibrium regime for longer t_w, so the maximum in the $TRM-ZTRM$ shifts towards longer observation times. The same appears to be true for the field dependence, exhibited in the main body of Fig. 9, the system after a longer waiting-time can sustain a stronger perturbation and still remain in the quasiequilibrium regime.

This similarity between the effects of the observation time and the field change can be naturally explained within the mean-field picture. The weak ergodicity breaking scenario mentioned in Sec. II A suggests that, as the observation time increases, the system can evolve very far from the state at time t_w, with the minimum correlation set by $q_{min}(H)$. Chaotic nature of the spin-glass state with respect to magnetic field, discussed in Sec. II B, forces the new *equilibrium* configuration after a small field change to have the minimum overlap $q_{min}(H)$ with the old configuration. Thus, both an increasing observation time and an increasing field change make the spin-glass state less correlated with the state at time t_w.

It is of interest to examine the waiting-time dependences of ΔH_1 and ΔH_2 for the two ''competing'' descriptions of spin-glass dynamics: the droplet model and the phase-space picture.

In the droplet model,[32] if $R(t_w)$ is an average droplet size and L_τ is an observation length scale, two limiting cases can be distinguished. For $R(t_w)\ll\xi_H$, the FDT is violated when $L_\tau\sim R(t_w)$, and the field does not play a significant role. For $\xi_H\ll R(t_w)$, the FDT is violated as soon as $L_\tau\sim\xi_H$, and the waiting-time is relatively unimportant. These regimes correspond approximately to the experimental regimes with $\Delta H<\Delta H_1$ and $\Delta H>\Delta H_2$, as discussed above. There is also an intermediate regime with $R(t_w)\sim\xi_H$. This regime is very interesting physically, because violation of the FDT depends on interplay among all three length scales: $L_\tau\sim R(t_w)\sim\xi_H$. Unfortunately, no predictions for this regime are given within the droplet model.[32] It has been argued[12] that, if a crossover between linear and nonlinear regimes is defined by a condition $R(t_w)=\xi_H$, the field change, needed to provoke nonlinear relaxation, should decrease with increasing t_w. This argument can explain the waiting-time dependence of ΔH_2. However, it fails in the case of ΔH_1, which *increases* with t_w. Therefore, the experimentally observed waiting-time dependence of ΔH_1 appears rather counterintuitive within the droplet scenario.

The phase-space picture of spin-glass dynamics does provide a consistent explanation for these phenomena. In this approach, evolution of a system in the phase space can be viewed as a series of transitions among traps, separated by free-energy barriers.[14] As the system equilibrates, it encounters traps with higher barriers, and these traps increasingly resemble the pure states, contributing to equilibrium.[15] The quasiequilibrium relaxation regime at short observation times corresponds to evolution within each trap, and the subsequent nonequilibrium behavior is related to evolution from trap to trap. As the waiting time t_w increases, the system has to overcome a higher effective barrier to leave a trap. This takes a longer time, or (if the observation time is fixed) a larger field change. Therefore, the characteristic field change for the weak linear-response violation, ΔH_1, increases with

t_w. However, after overcoming a higher barrier, the system can explore a broader free-energy landscape due to hierarchical structure of the phase space. It takes less time or a smaller field change to produce a state very different from the one at t_w. The nonequilibrium behavior is thus more affected by external perturbations for longer waiting-times. Therefore, the characteristic field change for the strong linear-response violation, ΔH_2, decreases with t_w.

Our results demonstrate that the transition from the quasiequilibrium to the nonequilibrium regime is better defined after longer waiting-times, both as a function of the observation time and as a function of the field change. This conclusion agrees with results of numerical simulations, which show the same effect when susceptibility is studied as a function of correlation.[17]

D. Scaling of the remanent magnetization

It was shown in Sec. III A that the equivalence of the TRM and the $MFC-ZFC$ breaks down already at $\Delta H_1(T)$, which, even at relatively short observation times, is only 10% of the corresponding AT field. Nonlinearity in response, however, can be observed for any field changes below $\Delta H_1(T)$. In this case, the ZFC magnetization is linear in magnetic field, but the $TRM=MFC-ZFC$ is nonlinear due to the influence of the field-cooled state.[37]

We argued in Sec. II A that the mean-field theory of aging phenomena predicts the $H/H_{AT}(T)$ scaling of the remanent susceptibility, $\chi_{FC}(H)-\chi_{ZFC}(T)$, if two additional assumptions are made. First, the master curve $\tilde{\chi}(C)$ should allow a linear approximation. Second, the minimum correlation $q_{min}(H)$ should be a homogeneous function of the field.

In order to see whether the first assumption is reasonable we determined the master curve $\tilde{\chi}(C)$ according to the method of Cugliandolo et al.[21] If the zero-field-cooled susceptibility is measured at the limit of validity of the FDT, the corresponding correlation $C(T)$ can be obtained from Eq. (9). Then the values of $\chi_{ZFC}(T)$ for different temperatures, plotted vs $C(T)$, span the master curve $\tilde{\chi}(C)$. The experimental master curve is displayed in Fig. 10. The data points were taken in the interval from $T=2.4$ K to $T=15.0$ K at the same low field $H=\Delta H=16$ Oe. Each measurement was independent of the others, and included a quench from above the glass temperature.

Figure 10 demonstrates that the experimental dependence of $\tilde{\chi}$ on C is close to linear over a wide range of correlations. This justifies the assumption underlying Eq. (12) that the master curve $\tilde{\chi}(C)$ at relatively low C can be approximated by a straight line. Results of the combined susceptibility-correlation measurements lead to the same conclusion.[27]

The inset in Fig. 10 exhibits three lines. The AT critical line is the same as in Fig. 3. The second line gives temperature dependence of the position of the peak in $TRM(H)$, which we denote as $H_M(T)$. The third line corresponds to temperature dependence of the position of the peak in $(MFC-ZFC)(H)$, which we refer to as $H_m(T)$. These peaks are easier to identify than the AT line itself. We shall use both $H_M(T)$ and $H_m(T)$, which are proportional to the AT field, as scaling parameters. Note that $\Delta H_1<\Delta H_2\approx H_m<H_M$.

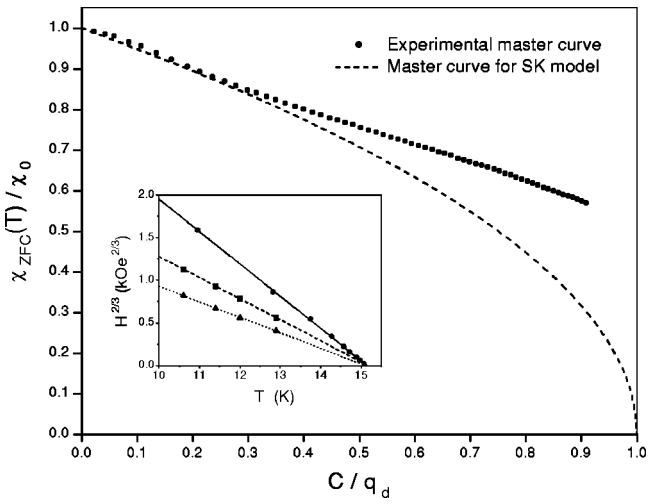

FIG. 10. The master curve $\tilde{\chi}(C)$ for the single-crystal Cu:Mn (1.5 at. %), estimated from the experimental $\chi_{ZFC}(T)$ dependence. The master curve for the SK model is $\tilde{\chi}=(1-C)^{1/2}$. The inset shows, from top to bottom $H_{AT}(T)$, the experimental AT line; $H_M(T)$, the position of the peak in $TRM(H)$; and $H_m(T)$, the position of the peak in $(MFC-ZFC)(H)$.

The experimental form for the AT line suggests that, to the leading order of magnitude, $q_{min}(H)\propto H^{2/3}$. Therefore, $q_{min}(H)$ is indeed a homogeneous function of order $p=2/3$, and the assumption underlying Eq. (13) is also verified.

Figure 11 exhibits field dependence of the remanent magnetization $(MFC-ZFC)(H)$, measured for different temperatures in the interval $T/T_g=0.7$–0.85. The curves are

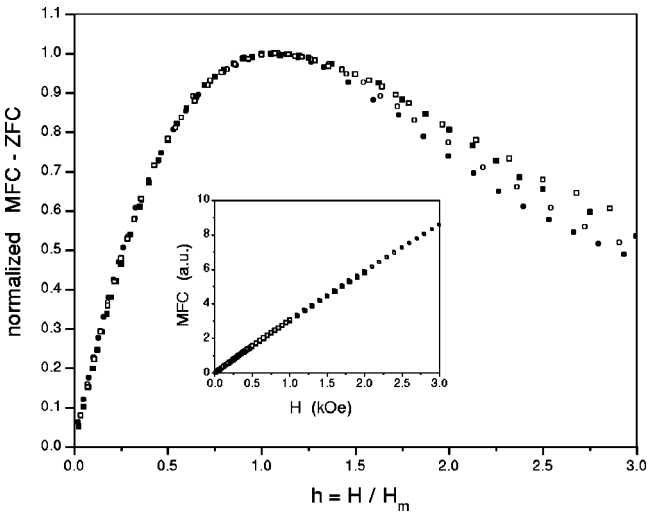

FIG. 11. Scaling of the remanent magnetization curves for different temperatures $T_r=T/T_g$. All the curves are for the single-crystal Cu:Mn (1.5 at. %). Solid circles: $T_r=0.70$, $H_m=750$ Oe; open circles: $T_r=0.75$, $H_m=550$ Oe; solid squares: $T_r=0.79$, $H_m=420$ Oe; open squares: $T_r=0.85$, $H_m=260$ Oe. The positions of the peaks, $H_m(T)$, are used as scaling parameters. The inset exhibits the corresponding field-cooled magnetization curves.

plotted versus $h=H/H_m(T)$, and normalized by one at $h=1$. All data points were taken at the same short observation time $\tau=40$ s with zero waiting-time. One can see that the quality of scaling is very good for $h<1$, i.e., within the linear-response regime. The scaling, however, deteriorates as the AT line corresponding to $h\approx 3.5$ is approached. This may be attributed to effects of the transverse freezing[35] on the longitudinal irreversibility, which are more pronounced at higher temperatures and higher fields.

The inset in Fig. 11 displays field dependence of the field-cooled magnetization for the same measurement temperatures. The data are presented as taken, without any rescaling of the field or adjustment of the magnetization magnitude. It is evident that the $MFC(H)$ is virtually independent of temperature. This means that the Parisi-Toulouse approximation[26] works well in the case of the Cu:Mn (1.5 at. %) sample.

The scaling of the remanent magnetization curves in Fig. 11 suggests that the master curve $\tilde{\chi}(C)$ in Fig. 1 is universal, that is, T and H independent. It would be interesting to see, therefore, if this curve depends on the choice of sample. Different spin-glass samples have different microscopic properties, and consequently, different magnetic-field scales. If the Parisi-Toulouse approximation holds, the magnetic field H appears in the analysis through $q_{min}(H)$ only. Therefore, if the master curve $\tilde{\chi}(C)$ is sample independent, and $q_{min}(H)$ has always the same functional form, we can expect the scaling of magnetization curves to hold for different samples.

In order to study this issue, we have measured the field-cooled and the thermoremanent magnetizations as functions of $H=\Delta H$ for five different spin-glass samples. In addition to the single crystal Cu:Mn (1.5 at. %), described previously, we have used a single-crystal Cu:Mn (0.6 at. %), with the glass temperature of about 6.0 K. Both samples have been prepared in Kammerlingh Onnes Laboratory (Leiden). Similar single crystals have been used for neutron-scattering experiments.[38] The other three of our samples are polycrystalline. The polycrystal Cu:Mn (6.0 at. %) has been extensively studied before.[8] Its glass temperature is near 31.0 K. The thiospinel $CdCr_{1.7}In_{0.3}S_4$ is an insulating short-range spin glass with $T_g=16.7$ K. It has also been studied in detail.[9] The second thiospinel sample, used in our analysis, has been obtained from the part of the first sample by sifting it through a 100 nm mesh. This was done to probe the finite-size effects.[39] The sifted thiospinel has a slightly lower glass temperature $T_g\approx 16.5$ K.

Figure 12 displays field dependence of the thermoremanent magnetization $TRM(H)$ for five spin-glass samples. The curves are plotted versus $h=H/H_M$, and normalized by one at $h=1$. All data points were taken at the same short observation time $\tau=90$ s after a field change, following a waiting-time of 30 min. The overall scaling in Fig. 12 is very impressive considering the diversity in properties of these spin glasses. The major departures from perfect scaling appear to result from finite-size effects. The inset in Fig. 12 exhibits scaling of the field-cooled magnetization curves

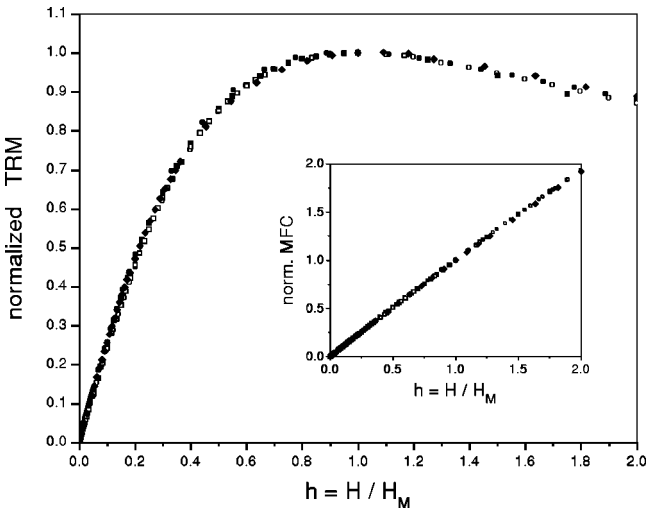

FIG. 12. Scaling of the thermoremanent magnetization curves for different spin-glass samples. Solid circles: polycrystal of thiospinel ($T_r=0.86$, $H_M=45$ Oe); Open circles: sifted polycrystal of thiospinel ($T_r=0.86$, $H_M=50$ Oe); solid squares: single crystal Cu:Mn (0.6 at. %) ($T_r=0.80$, $H_M=200$ Oe); open squares: polycrystal of Cu:Mn (6.0 at. %) ($T_r=0.83$, $H_M=300$ Oe); solid diamonds: single crystal of Cu:Mn (1.5 at. %) ($T_r=0.80$, $H_M=550$ Oe). The positions of the peaks, $H_M(T)$, are used as scaling parameters. The inset displays scaling of the corresponding field-cooled magnetization curves.

$MFC(H)$. The scaling is also good, suggesting that the functional forms of $q_{min}(H)$ are similar for different samples.

The results in Fig. 12 may be interpreted as indication of the fact that the master curve $\tilde{\chi}(C)$ in Fig. 1 is essentially sample independent. Thus, there is universality for the magnetic properties of different spin-glass systems.

The magnetization scaling in spin glasses has been observed before, most notably by Bouchiat and Monod,[40] who carried out the first systematic study of the remanent magnetization. However, each magnetization curve in their analysis included only six data points, and the curves were found to scale ''to better than $\pm 10\%$'' (Ref. 40). Temperature dependence of the scaling parameter was fitted using an exponential approximation, $H_{max}(T)\propto\exp(-\beta T/T_g)$, and the results were discussed in terms of the Néel model for an assembly of magnetic particles.[40]

The contribution of the present paper is twofold. First, we show that the scaling of the remanent magnetization holds with remarkable accuracy, at least within the linear-response regime. The magnetization curves for metallic and insulating spin glasses are also found to scale together. Second, our results demonstrate that the scaling parameters, $H_m(T)$ and $H_M(T)$, have the same temperature dependence as the AT critical field: $H_m(T)\propto H_{AT}(T)\propto(1-T/T_g)^{3/2}$. We argue that the H/H_{AT} scaling of the remanent magnetization can be derived from the mean-field dynamics. Thus, the observed scaling supports predictions of the mean-field theory of aging phenomena. It also provides important information about properties of $\chi(C)$ in the aging regime.

IV. CONCLUSION

Violation of the fluctuation-dissipation theorem is one of the most important features of spin-glass dynamics. In traditional relaxation experiments, this violation is studied as a function of observation time. In the present paper, we probe it as a function of an increasing field change ΔH by measuring ''irreversibility of the irreversibility,'' $TRM-(MFC-ZFC)$. This quantity slowly deviates from zero as the observation time increases. Because linear field scale corresponds to logarithmic time scale, significant departures of the $TRM-(MFC-ZFC)$ from zero can be observed at relatively low ΔH. Our experiments show that linear-response violation lines in $(T,\Delta H)$ plane have the same functional form as the de-Almeida–Thouless critical line. This conclusion is further supported by measurements of the effective waiting-time t_w^{eff} and analysis of waiting-time effects. Our results suggest that there is a fundamental link between static and dynamic properties of spin glasses, predicted by the mean-field theory of aging phenomena.

We also argue that the H/H_{AT} scaling for the remanent magnetization can be derived from the mean-field picture of spin-glass relaxation, if two additional assumptions are made. These assumptions are verified experimentally. The scaling of the magnetization curves is shown to be very accurate, both for different temperatures and different samples. These results suggest that the mean-field theory of aging phenomena correctly describes magnetic-field effects on spin-glass dynamics.

ACKNOWLEDGMENTS

We would like to thank Professor J. A. Mydosh for providing us with the Cu:Mn single-crystal samples, prepared in Kamerlingh Onnes Laboratory (Leiden, The Netherlands). We are most grateful to Dr. J. Hammann and Dr. E. Vincent from CEA Saclay (France) for giving us one half of their thiospinel sample.

[1] M. Mezard, G. Parisi, and M.A. Virasoro, *Spin Glass Theory and Beyond* (World Scientific, Singapore, 1987).
[2] D. Sherrington and S. Kirkpatrick, Phys. Rev. Lett. **35**, 1792 (1975).
[3] J.R.L. de Almeida and D.J. Thouless, J. Phys. A **11**, 983 (1978).
[4] E. Marinari, G. Parisi, F. Ricci-Tersenghi, J.J. Ruiz-Lorenzo, and F. Zuliani, J. Stat. Phys. **98**, 973 (2000).
[5] S. Caracciolo, G. Parisi, S. Patarnello, and N. Sourlas, Europhys. Lett. **11**, 783 (1990); E.R. Grannan and R.E. Hetzel, Phys. Rev. Lett. **67**, 907 (1991); J.C. Ciria, G. Parisi, F. Ritort, and J.J. Ruiz-Lorenzo, J. Phys. I **3**, 2207 (1993).
[6] E. Marinari, G. Parisi, and F. Zuliani, J. Phys. A **31**, 1181 (1998).
[7] F. Krzakala, J. Houdayer, E. Marinari, O.C. Martin, and G. Parisi, Phys. Rev. Lett. **87**, 197204 (2001).
[8] G.G. Kenning, D. Chu, and R. Orbach, Phys. Rev. Lett. **66**, 2923 (1991).
[9] F. Lefloch, J. Hammann, M. Ocio, and E. Vincent, Physica B **203**, 63 (1994), and references therein.
[10] J. Mattsson, T. Jonsson, P. Nordblad, H.A. Katori, and A. Ito, Phys. Rev. Lett. **74**, 4305 (1995).
[11] D. Petit, L. Fruchter, and I.A. Campbell, Phys. Rev. Lett. **83**, 5130 (1999).
[12] G.J.M. Koper and H.J. Hilhorst, J. Phys. (France) **49**, 429 (1988).
[13] M. Lederman, R. Orbach, J. Hammann, M. Ocio, and E. Vincent, Phys. Rev. B **44**, 7403 (1991); J. Hammann, M. Lederman, M. Ocio, R. Orbach, and E. Vincent, Physica A **185**, 278 (1992).
[14] J.-P. Bouchaud, J. Phys. I **2**, 1705 (1992); E. Vincent, J.-P. Bouchaud, D.S. Dean, and J. Hammann, Phys. Rev. B **52**, 1050 (1995).
[15] L.F. Cugliandolo and J. Kurchan, Phys. Rev. Lett. **71**, 173 (1993); J. Phys. A **27**, 5749 (1994); Philos. Mag. B **71**, 501 (1995).
[16] J.-P. Bouchaud, L. F. Cugliandolo, J. Kurchan, and M. Mezard, in *Spin Glasses and Random Fields*, edited by A.P. Young (World Scientific, Singapore, 1997).
[17] S. Franz and H. Rieger, J. Stat. Phys. **79**, 749 (1995).
[18] E. Marinari, G. Parisi, F. Ricci-Tersenghi, and J.J. Ruiz-Lorenzo, J. Phys. A **31**, 2611 (1998).
[19] S. Franz, M. Mezard, G. Parisi, and L. Peliti, Phys. Rev. Lett. **81**, 1758 (1998); J. Stat. Phys. **97**, 459 (1999).
[20] G. Parisi, Nuovo Cimento D **20**, 1221 (1998).
[21] L.F. Cugliandolo, D.R. Grempel, J. Kurchan, and E. Vincent, Europhys. Lett. **48**, 699 (1999).
[22] R. Kubo, Rep. Prog. Phys. **29**, 255 (1966).
[23] L.P. Levy and A.T. Ogielski, J. Math. Phys. **30**, 683 (1989).
[24] M. Ocio, H. Bouchiat, and P. Monod, J. Phys. (France) Lett. **46**, L647 (1985).
[25] J.O. Andersson, J. Mattsson, and P. Svedlindh, Phys. Rev. B **46**, 8297 (1992).
[26] G. Parisi and G. Toulouse, J. Phys. (France) Lett. **41**, L361 (1980); J. Vannimenus, G. Toulouse, and G. Parisi, J. Phys. (France) **42**, 565 (1981).
[27] D. Herisson and M. Ocio, cond-mat/0112378 (unpublished).
[28] F.T. Bantilan and R.G. Palmer, J. Phys. F: Met. Phys. **11**, 261 (1981).
[29] G. Parisi, Phys. Rev. Lett. **50**, 1946 (1983); Physica A **124**, 523 (1984).
[30] I. Kondor, J. Phys. A **22**, L163 (1989).
[31] F. Ritort, Phys. Rev. B **50**, 6844 (1994); Philos. Mag. B **71**, 515 (1995).
[32] D.S. Fisher and D.A. Huse, Phys. Rev. B **38**, 373 (1988); **38**, 386 (1988).
[33] P. Nordblad, L. Lundgren, and L. Sandlund, J. Magn. Magn. Mater. **54-57**, 185 (1986); L. Lundgren, P. Nordblad, and L. Sandlund, Europhys. Lett. **1**, 529 (1986).
[34] C. Djurberg, J. Mattsson, and P. Nordblad, Europhys. Lett. **29**, 163 (1995).
[35] M. Gabay and G. Toulouse, Phys. Rev. Lett. **47**, 201 (1981); D.M. Cragg, D. Sherrington, and M. Gabay, *ibid.* **49**, 158 (1982).
[36] L.E. Wenger and J.A. Mydosh, Phys. Rev. B **29**, 4156 (1984).
[37] P. Nordblad, L. Lundgren, and L. Sandlund, Europhys. Lett. **3**, 235 (1987).
[38] F.J. Lamelas, S.A. Werner, S.M. Shapiro, and J.A. Mydosh, Phys. Rev. B **51**, 621 (1995).
[39] T.L. Swan, R. Orbach, G.G. Wood, Y.G. Joh, J. Hammann, and E. Vincent, Bull. Am. Phys. Soc. **45**, 979 (2000).
[40] H. Bouchiat and P. Monod, J. Magn. Magn. Mater. **30**, 175 (1982).